TISSUE ENGINEERING: Part A
Volume 26, Numbers 21 and 22, 2020

DOI: 10.1089/ten.tea.2020.0068

termis
Tissue Engineering
& Regenerative Medicine
International Society

ORIGINAL ARTICLE

In Vivo-Like Morphology of Intercalated Discs Achieved in a Neonatal Cardiomyocyte Culture Model

Ailin Wei, BS,[1] Zhonghai Wang, PhD,[1] Albert Luca Rancu,[2] Zongming Yang, BS,[1] Shenghao Tan,[1] Thomas Keith Borg, PhD,[3] and Bruce Zhi Gao, PhD[1]

In vitro cultures to be used in various analytical investigations of cardiomyocyte (CM) growth and function for enhancing insight into physiological and pathological mechanisms should closely express *in vivo* morphology. The aim of the studies is to explore how to use microfabrication and physical-cue-addition techniques to establish a neonatal rat CM culture model that expresses an end-to-end connected rod shape with *in vivo*-like intercalated discs (ICDs). Freshly isolated neonatal rat CMs were cultured on microgrooved polydimethylsiloxane substrate. Cell alignment and ICD orientation were evaluated using confocal fluorescence and transmission electron microscopy under various combinations of different culture conditions. Cyclic stretch and blebbistatin tests were conducted to explore mechanical and electrical effects. Laboratory-made MATLAB software was developed to quantify cell alignment and ICD orientation. Our results demonstrate that the mechanical effect associated with the electrical stimulation may contribute to step-like ICD formation viewed from the top. In addition, our study reveals that a suspended elastic substrate that was slack with scattered folds, not taut, enabled CM contraction of equal strength on both apical and basal cell surfaces, allowing the cultured CMs to express a three-dimensional rod shape with disc-like ICDs viewed cross-sectionally.

Keywords: cardiac cell culture model, neonatal rat cardiomyocytes, intercalated disc, electrical stimulation, mechanical stretch

Impact Statement

In this article, we describe how the tugging forces generated by cardiomyocytes (CMs) facilitate the formation of the morphology of the intercalated discs (ICDs) to achieve mechanoelectrical coupling between CMs. Correspondingly, we report experimental techniques we developed to enable the *in vivo*-like behavior of the tugging forces to support the development of *in vivo*-like morphology in ICDs. These techniques will enhance insight into physiological and pathological mechanisms related to the development of tissue-engineered cardiac constructs in various analytical investigations of CM growth and function.

Introduction

In heart tissue, cardiomyocytes (CMs) express a rod-like shape and are connected end to end (with some branches) to form a long contractile muscle fiber. The entire region of the end-to-end abutment between CMs consists of intercalated discs (ICDs), unique structures that exist only in the myocardium. The major function of the ICDs is to facilitate mechanical and electrical coupling between adjacent CMs through cellular junctions distributed at ICDs. These cellular junctions include fascia adherens (FA) with cell/cell adhesion molecules such as N-cadherin, which serves as a cellular adhesion junction to connect myofibrils in adjacent cells for force transmission.[1]

The functions of the ICD components depend heavily on ICD morphology. The most typical features of ICDs, commonly found in working ventricular myocardium of adult higher vertebrates, are that (1) viewed along the longitudinal axis of the CMs, they display a disk morphology and (2) viewed laterally, they exhibit a step-like morphology with ''treads'' and ''risers,'' respectively, perpendicular to and in parallel with the longitudinal axis. The tread segments,

[1]Department of Bioengineering, Clemson University, Clemson, South Carolina, USA.
[2]Duke University, Durham, North Carolina, USA.
[3]Department of Regenerative Medicine, Medical University of South Carolina, Charleston, South Carolina, USA.

which are at the interfaces between two end-to-end connecting CMs, typically have a pleated appearance.[2] The riser sections of ICDs lie at the interface between two side-to-side contacting CMs.

To ensure that engineered cell constructs retain myocardial function, especially the electrically activated mechanical contraction,[3] an *in vivo*-like electromechanical coupling between CMs must be achieved.

Aligned CM elongation and end-to-end CM connection must be formed at first. According to the literature, the most effective method for creating CM alignment is topographic patterning, which is classified into four categories: (1) microabrasion[4]; (2) microcontact printing[4–6]; (3) microgroove guidance[7–9]; and (4) biomimetic microwrinkle guidance.[10] Polydimethylsiloxane (PDMS) is a fully characterized biocompatible material[11] and has been widely used to achieve CM alignment. PDMS-based methods to achieve cell alignment have mostly been applied in categories 2, 3, and 4. Microgrooves are advantageous because they are easy to use, consist of geometry and physical conditions, and maintain their integrity throughout the life of the cell culture. More importantly, only in the microgroove method can the compliance of the PDMS substrate be adjusted. Consequently, we chose this method for CM alignment. Note that in most of the studies reported in the literature, PDMS substrates were not suspended: Cells were cultured on PDMS bound to a hard surface.

Achieving only end-to-end CM alignment (which has been accomplished by various methods[12]) in an *in vitro* CM culture is not sufficient to study mechanical interaction between adjacent cells. In this study, we report our research results of promoting an *in vivo*-like ICD formation in an aligned CM culture model, which includes a microgrooved PDMS substrate to achieve CM alignment.

Materials and Methods

Fabrication of microgrooved polydimethylsiloxane with tunable Young's modulus

Microgrooved PDMS was fabricated using soft lithography techniques (Fig. 1A). Grooves with depths of 0.5 ± 0.2, 1.5 ± 0.2, and $5 \pm 0.2\,\mu m$ (with a calibrated machine accuracy of $0.2\,\mu m$) were studied. Our study showed that (data not shown) transverse contacts of CMs began to fail to be achieved at a groove depth of around $5\,\mu m$, as Motlagh *et al.* showed in a similar study.[8] Transverse contacts are necessary for gap junction formation and thus for the synchronized contraction of the culture. Our unshown results also indicated that $0.5\,\mu m$ grooves were not deep enough to guide CM alignment. In our CM alignment assessment, results on $1.5\,\mu m$ deep grooves were statistically comparable to those observed in *in vivo* tissue. Consequently, $1.5 \pm 0.2\,\mu m$ grooves were used in the experiments reported in this study. The thickness of the PDMS substrate used for this study was $180 \pm 10\,\mu m$.

In this study, PDMS substrates with two values of Young's modulus were prepared: 1.72 MPa and 130 kPa.[13] The Young's modulus most commonly used for PDMS is 1.72 MPa; Young's modulus of a normal heart is at the level of 10 kPa.[14] Practically, 130 kPa is the minimal Young's modulus at which we can repeatedly produce identical grooves for experimental design. In addition, a too-soft substrate cannot be used to achieve the stretching described later. The 130 kPa PDMS substrate was tuned by mixing Sylgard 527 gel (Sylgard 527; Dow Corning) and Sylgard 184 gel at different mass ratios (5:1). The Young's modulus of the PDMS substrate was monitored with a material testing machine (Instron). The PDMS substrate (membrane) was glued with fresh liquid PDMS to a PDMS frame (a 4-mm-thick rectangular frame with an internal dimension of 60 mm length, 16 mm width, and 3.5 mm height) cast from a machined acrylic mold to form a cell culture chamber (referred to hereafter as ''chamber'').

After gluing the PDMS substrate, we immediately added water to the top of the membrane to create an excess membrane area (the area of the membrane was larger than the area of the bottom of the chamber frame), as shown in Figure 2A and B. Excess areas created by water with a volume of $500\,\mu L$, 1 mL, and 2 mL were studied; a substrate created by water with a volume of $500\,\mu L$ was used in the experiments since it produced the most confluent layer of cell culture.

Compliance (the inverse of stiffness) is mainly determined by Young's module of the PDMS and the geometry of the PDMS substrate. Due to the complexity of the geometry, we used a custom-defined effective stiffness to quantify the system's compliance. The effective stiffness was defined as the force exerted by the medium divided by the average PDMS deformation. We explored the compliance by filling a chamber with water, as shown in Figure 2C. The chamber was covered with a coverglass with a gap for pipetting water until the entire chamber was filled and the gap closed. The force (F) was the weight of the water with a density of ρ, which was calculated from the volume (V) of the filled chamber through $F = \rho \times V \times g$. The average PDMS deformation (Δd) was estimated by dividing the volume of excess water (ΔV, the filled volume subtracted by the chamber volume, 3.4 mL) by the inner cross-sectional area of the chamber ($A = 10\,cm^2$) through $\Delta d = \Delta V/A$. The effective stiffness of 130 kPa substrate created by the addition of water in the amounts of $500\,\mu L$, 1 mL, and 2 mL and of 1.72 MPa substrate created with $500\,\mu L$ water was evaluated, as its definition through $k = F/\Delta d$ and is shown in Table 1.

Tissue collection, cell isolation, and culture

Four-week-old adult male and Day 3 neonatal Sprague-Dawley rats were euthanized to collect heart tissues according to procedures approved by the Clemson University Institutional Animal Care and Use Committee (protocol nos. AUP2017-069 and AUP2016-042). The procedure conforms to the Guide for the Care and Use of Laboratory Animals (NIH Publication, 8th Edition, 2011). Ventricular CMs were isolated from the neonatal rat hearts using a 2-day protocol, as described in our previous publication.[15] Meanwhile, PDMS culture chambers were autoclaved and coated with freshly prepared fibronectin solution ($20\,\mu g/mL$) (Sigma-Aldrich) overnight. After the fibronectin solution was aspirated off, the coated PDMS substrate was rinsed once with the warm medium. CMs were then seeded at 1.5×10^6 cells per chamber. The cells were cultured at 37°C with 5% CO_2 in Dulbecco's modified Eagle's medium (Gibco) supplemented with 1% antibiotic/antimycotic (Gibco) and 10% fetal bovine serum (Sigma-Aldrich). Cells were allowed to attach to the substrate for 1 day. The medium was replaced

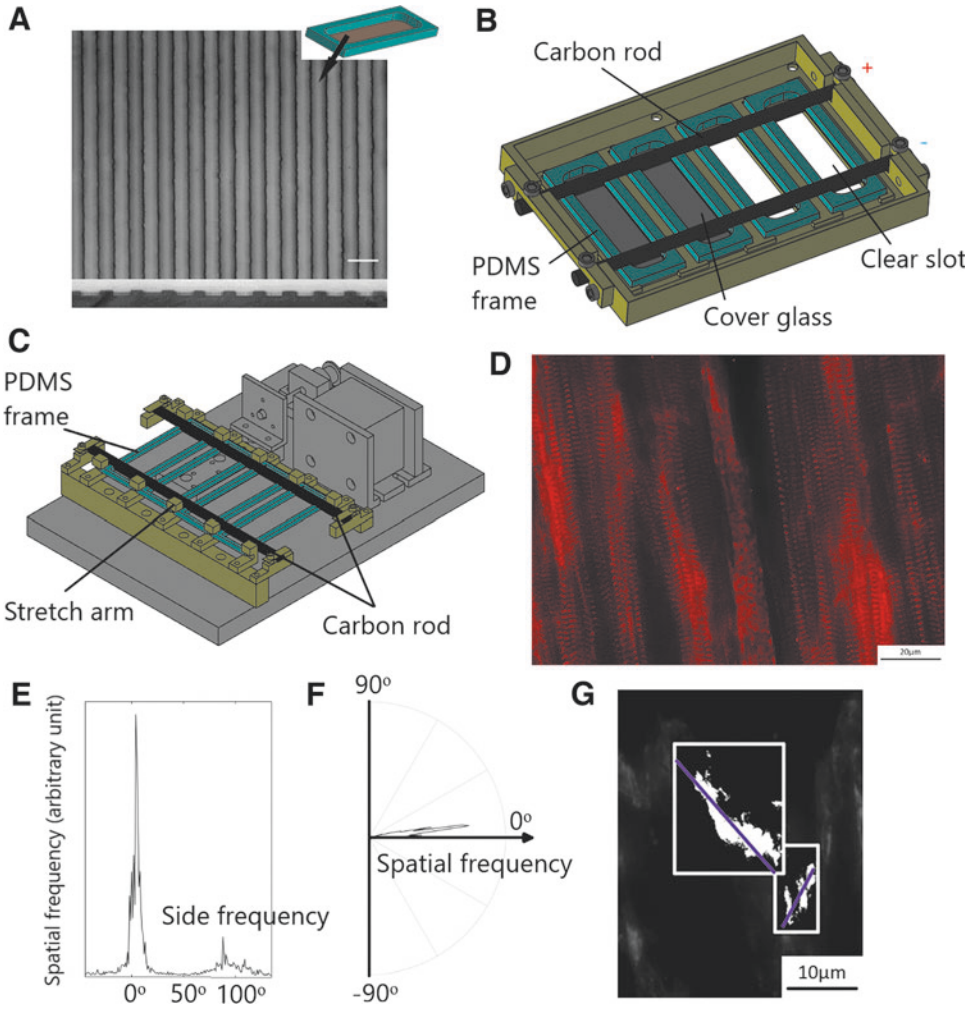

FIG. 1. CM culture apparatus and analysis method. **(A)** Phase images of the microfabricated grooved substrate: *upper panel*: *top view*; *bottom panel*: *cross-sectional view*. Scale bar = 20 μm. **(B)**CM culture device with electrical stimulation: Four PDMS cell culture chambers (Only frames [cyan] shown). Submersible protrusions on *black carbon bars* served as electrodes in CM culture medium. **(C)** The cyclic stretcher: On a single side only, *green* segments were driven by the motor system to stretch the four PDMS chambers. **(D)** CM alignment and ICD orientation analyzed using the immunofluorescence staining images of the cardiac cells (only α-actinin staining shown here). Scale bar = 20 μm. **(E)** CM alignment as an orientation spectrum obtained from D. **(F)** With the removal of the side frequency, the orientation spectrum in a polar coordinate system. **(G)** ICD orientation analyzed by first selecting an ROI (*white rectangular frames*), then conducting binarization inside ROI using a threshold of 85% highest *gray* level; ICD orientations obtained by fitting the binarized data to a *straight line* (*purple*) and calculating the slope of the line. Scale bar = 10 μm. CM, cardiomyocyte; ICD, intercalated disc; PDMS, polydimethylsiloxane; ROI, region of interest.

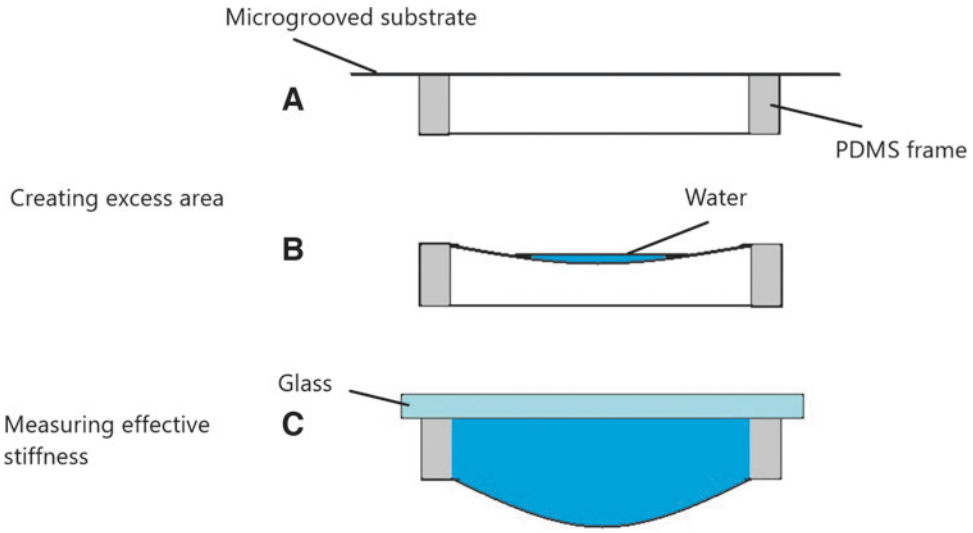

FIG. 2. **(A, B)** Creating an excess membrane area. **(C)** Measuring effective stiffness.

Table 1. Evaluation of the Substrate's Effective Stiffness (Mean ± Absolute Error from Three Samples)

Membrane	*Volume of water filling chamber (V, mL)*	*Volume of excess water (ΔV, mL)*	*Force exerted by water filling chamber (F, 10^{-2} N)*	*Average deformation (Δd, cm)*	*Effective stiffness (k, N m^{-1})*
130 kPa with 500 μL	5.9 ± 0.9	2.5 ± 0.9	5.9 ± 0.9	0.25 ± 0.09	24 ± 7
130 kPa with 1 mL	6.8 ± 0.8	3.4 ± 0.8	6.8 ± 0.8	0.34 ± 0.08	20 ± 3
130 kPa with 2 mL	8.5 ± 0.6	5.1 ± 0.6	8.5 ± 0.6	0.51 ± 0.06	17 ± 1
1.72 MPa with 500 μL	4.5 ± 0.5	1.1 ± 0.5	4.5 ± 0.5	0.11 ± 0.05	40 ± 26

1 day after cell seeding, and unattached cells were rinsed off. The medium was replaced every 36 h after that.

Electrical stimulation device

In this study, a polyetheretherketone (PEEK) culture box was constructed with four slots with open bottoms (Fig. 1B). Four PDMS chambers were placed on the box, each chamber at one of the four slots. The bottom of each chamber could be suspended due to the opening at the bottom of each slot (e.g., the two white slots, Fig. 1B) or be seated on a coverglass placed on a slot to close the opening (e.g., the gray bottom slots in Fig. 1B). Electrical stimulation was achieved by using two pure carbon bars (Ladd Research Industries) mounted on the culture box; the bars were machined so that their protrusions were submerged in the medium to serve as electrodes. The carbon bars were cabled to the stimulator, which comprised a stimulation-signal generator (STG1008; Multichannel Systems) and a power amplifier (model UT01; Marchand Electronics). Cells were stimulated with a biphasic pulse (1 ms "+ pulse" followed by 1 ms "− pulse") train (1 Hz) at 3.6 peak-peak V/cm.

Cyclic stretch device

After cells had been seeded for 3 or 24 h, the chambers were moved to the stretch device (Fig. 1C), custom-built to stretch four chambers. The chambers were suspended on the stretcher arms with hooks mounted on a PEEK base. Carbon bars were mounted on the stretcher arms for electrical stimulation, as described above. A stepper motor was used to drive the stretcher arms. A cyclic stretch program was designed to achieve a 0.3 s triangular wave stretch (linear speed back and forth) at 5% stretch magnitude or 0.5 s similar stretch at 10% stretch magnitude. The mechanical strains (i.e., 5% and 10%) were calibrated when the substrate was mounted on the PDMS frames and with the confluent cell culture. Both conditions included a 0.7 s relaxed stage for each cycle. In the cyclic stretch, the longitudinal stretch was used: The direction of the stretch was parallel to the microgrooves, that is, in the direction of CM alignment. The chamber was stretched for a period of 5 or 6 days. In addition, electrical stimulation without mechanical stretch was provided to the chambers to study the difference between electrical-triggering-caused internal cell stretch and externally exerted mechanical stretch.

Immunofluorescence staining

Cells were fixed with 4% paraformaldehyde (pH 7.4) (Sigma-Aldrich) for 10 min, rinsed thoroughly with phosphate-buffered saline (PBS) (Sigma-Aldrich), penetrated with 0.25% Triton X-100 (Sigma-Aldrich) for 15 min and blocked with 10% (v/v) normal donkey serum (Sigma-Aldrich) at 4°C overnight. The myofibrils were labeled by α-actinin staining (mouse anti-α-actinin, 1:500; Sigma-Aldrich). Fascial adherents were labeled with N-cadherin staining (rabbit anti-pan cadherin, 1:200; Abcam). Secondary antibodies followed all primary antibodies: Alexa Fluor 488-conjugated donkey anti-rabbit IgG (H+L) (1:500; Jackson ImmunoResearch), Alexa Fluor 594-conjugated donkey anti-mouse IgG (H+L) (1:200; Jackson ImmunoResearch). Immunocytochemistry observation was conducted with Carl Zeiss Axiovert 200 m and a Leica TCS SPE confocal microscope for three-dimensional (3D) reconstruction.

Transmission electron microscopy

CM culture and heart tissue blocks were fixed with 2% glutaraldehyde (Electron Microscopy Sciences) in PBS for 30 min at room temperature. After fixation, CM culture and blocks were rinsed in PBS and postfixed in 1% osmium tetroxide (Sigma-Aldrich) in distilled water for 1 h. Cells were dehydrated in a serial gradient of ethanol; they were rinsed with ethanol/acetonitrile (ACN) (Sigma-Aldrich) mixtures with a serial ratio. Then, the CM culture was penetrated in ACN-PolyBed (Polysciences, Inc.) mixture with a serial ratio. The CM culture was penetrated with 100% PolyBed overnight and cured at 60°C in an oven for 48 h. A 90 nm section was cut with a Leica UltraCutR, and sections were placed on a copper grid (400 μm square) on a glass slide for staining. The staining was conducted with 2% uranyl acetate (Structure Probe, Inc., West Chester, PA, USA) for 40 min at 37°C in a dark room and 4% lead citrate (Sigma-Aldrich) for 4 min in a CO_2-free environment. Sections were desiccated overnight before imaging with JEOL transmission electron microscope (TEM) at 120 kV.

Blebbistatin test

Blebbistatin is an inhibitor used to inhibit myosin ATPase activity by suppressing actomyosin-based motility. Blebbistatin solution (10 μM) (Sigma-Aldrich) was applied to the CM culture chamber with 130 kPa suspended substrate with electrical stimulation.

Summary of different test groups

Eight different test groups are summarized in Table 2.

Table 2. Experimental Conditions for Each Test Group

Experimental test group	*Grooved substrate*	*Young's modulus of the substrate*	*Substrate suspension: suspended (√) or set on glass (X)*	*Electrical stimulation*	*Cyclic stretching*	*Blebbistatin*
Group 1 (G1)	X	1.72 MPa	X	X	X	X
Group 2 (G2)	√	1.72 MPa	X	X	X	X
Group 3 (G3)	√	1.72 MPa	√	√	X	X
Group 4 (G4)	√	130 kPa	√	X	X	X
Group 5 (G5)	√	130 kPa	X	√	X	X
Group 6-1 (G6)	√	130 kPa	√	√	X	X
Group 6-2	√	130 kPa	√	√	X	√
Group 7 (G7)	√	130 kPa	√	X	√	X
Group 8 (G8)	Heart tissue from adult rat					

Analysis

To characterize CM alignment and ICD orientation among different groups, 10 fields of view were arbitrarily selected from each culture chamber to record fluorescence images (e.g., Fig. 1D). Myofibril alignment, which is used to evaluate CM alignment in our study, was assessed through the stained α-actinin. A MATLAB Fourier transform program was developed to assess the alignment of myofibrils: From the spatial frequency, the corresponding alignment was calculated using the arctan function. For each image, the spatial frequency corresponding to the spectral pick (Fig. 1E) was selected to calculate the average myofibril alignment, referred to hereafter as the axis of CM alignment. The percentage of the alignment was calculated from the sum of the spectral components corresponding to the alignment direction within ±15°, ±20°, and ±30° of the average myofibril alignment divided by the total alignment spectrum. The percentage was used for quantifying CM alignment. When the myofibrils were linearly aligned (i.e., >70% aligned within ±15°), an extra band-pass filter was used to remove a side spatial frequency caused by the parallel myofibrils (Fig. 1E). Typically, this side frequency corresponded to a direction perpendicular to the average alignment. Therefore, the band-pass filter was designed to remove the orientation spectrum within ±15° centered at 90° of the axis of CM alignment (the pick spectrum). The percentage of the alignment was calculated after the removal of this side frequency from all spectra (e.g., Fig. 1F).

A second MATLAB program was developed to assess ICD orientation. Fluorescence images of stained N-cadherin were used for the analysis. First, regions of interest (ROIs) were selected manually to cover the transverse sections of arbitrarily selected ICD. Each ROI was binarized with a threshold of 85% of the highest gray level. The binarized image was linearly fitted, and the slope of the fit line was used as the orientation of the transverse ICD (Fig. 1G). To simplify the description, ICD orientation is used throughout this article without explicitly providing the slope. The angle between the axis of CM alignment and the ICD orientation were calculated and are defined here as the angle of ICD, which was presented with Rozeta software (Jacek Pazera) to provide a rose diagram. The percentage of step-like ICDs was calculated from the number of ICDs, whose angles were within ±30°, divided by the total number of ICDs.

Statistics

In total, 8 different test groups (G1–G8) were investigated. For each test group, multiple samples (e.g., identical culture chambers) were tested. Before data from different samples in the same test group were merged, Levene's test was used to assure equal variance could be assumed. For comparing differences among groups without normally distributed or equal variance, Kruskal–Wallis one-way analysis of variance (ANOVA) test followed by Tamhane's T2 test was used. For studying the difference between the two groups, we used Student's *t*-test for equal variance. For all tests, p-values of <0.05 were considered significant.

Results

Cell alignment

CM alignments were evaluated after 6 days in culture through Fourier transforming the fluorescence images of stained α-actinin (Supplementary Fig. S1). Figure 3 shows quantified cell alignments under the first six (G1–G6) and the last (G8) CM culture conditions listed in Table 1. Kruskal–Wallis one-way ANOVA test followed by Tamhane's T2 test when using the percentages of the alignment within ±30° of the direction of alignment of the average myofibril showed that (1) there were statistical differences between G1 and all other groups. Alignment in the random culture (G1) was significantly lower than that in G2 to G6 and in G8; (2) alignments under G4 and G5 were comparable to that in adult rat heart tissue (G8); (3) alignments under G2, G3, and G6 were slightly higher than alignment in G8 ($p > 0.05$).

Analysis of electrical stimulation

In our experiments, the excitation threshold (ET) was defined as the minimal voltage (vol) at which at least 85% of the cells were contracting synchronously. The data reported in this study were from only those cultures that did not have apparently synchronous contracting (<50%) before we applied electrical stimulation. Table 3 shows the measured ET ($n = 6$ from 3 cell isolations on 130 kPa suspended PDMS substrate). When cells were cultured on 130 kPa suspended PDMS substrate (G6), electrical stimulation of 3.6 vol/cm (1.8 vol for biphase) caused the entire membrane to contract with the cell construct, as shown in Supplementary Video

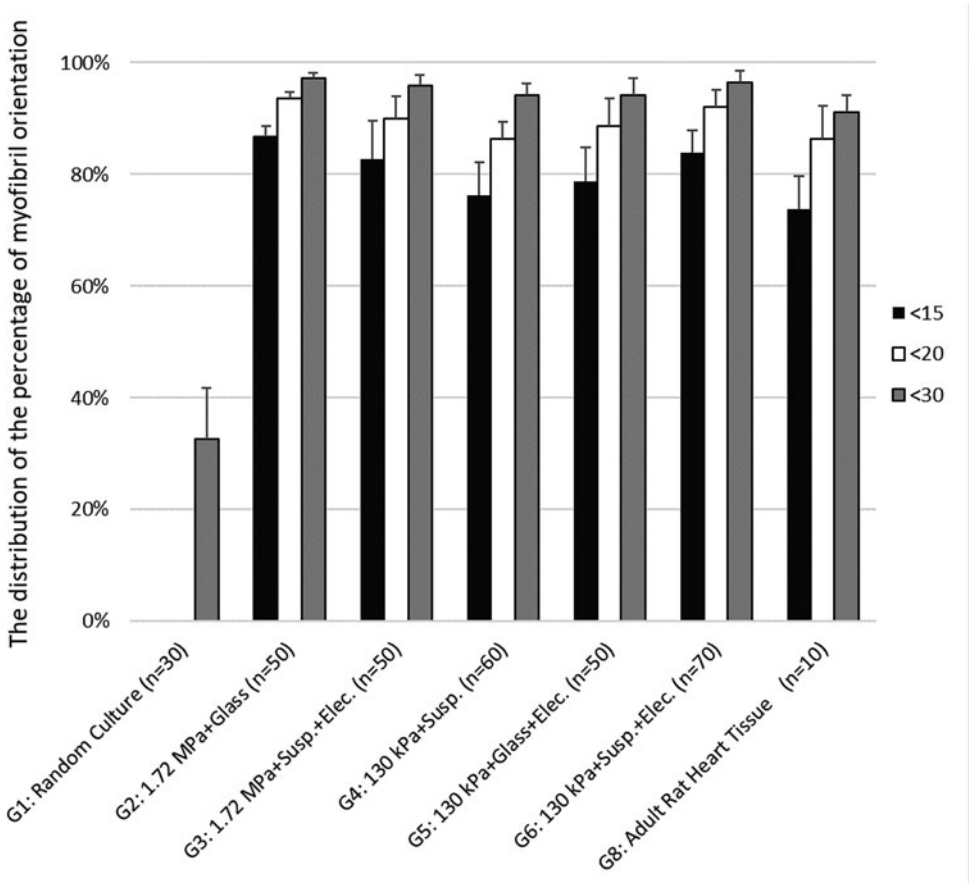

FIG. 3. The CM alignment assessment through the distribution of the percentage of myofibril alignment. From *left* to *right* are (G1) random culture, (G2) 1.72 MPa substrate attached on a coverglass without electrical stimulation, (G3) 1.72 MPa suspended substrate with electrical stimulation, (G4) 130 kPa suspended substrate without electric stimulation, (G5)130 kPa substrate attached on a coverglass with electrical stimulation, (G6) 130 kPa suspended substrate with electrical stimulation, and (G8) adult rat heart tissue.

S1. Electrical stimulation with 3.6 vol/cm also caused 75% CMs to contract synchronously on other test groups (G2, G3, and G5).

Immunofluorescence staining

ICD orientation was examined after 6 days in CM culture. Because at Day 6 *in vivo*-like CM alignment and ICD orientation were achieved, but gap junctions had not become mature, ICD alignment was visualized using N-cadherin staining, not Connexin 43 staining. The myofibrils were labeled by α-actinin staining to show their relationship to the ICDs. Visually, on 130 kPa suspended substrate with electrical stimulation (G6; Fig. 4A, B), a large number of ICDs was found to be perpendicular to the axis of CM alignment. This number was much higher than that on the 1.72 MPa substrate attached to a coverglass without electrical stimulation (G2; Fig. 4C, D). The angle of the ICDs was measured in cultures under G2 to G6. A Levene's test on ICD orientation on each sample showed that equal variance could be assumed between samples under all conditions. Thus, the data points for each test group were from different samples (e.g., data come from different culture chambers and different cell dissections) in the same statistical group (e.g., $n = 283$; Fig. 4E). The angular data processed with Rozeta software (Jacek Pazera) are presented as a rose diagram (Fig. 4E–J), and the percentage of step-like ICDs is summed in a bar plot (Fig. 4K).

The percentage of step-like ICDs in adult rat heart ventricle tissue (G8) was about 90%. The percentage of step-like ICDs for G6 (72.7%) was similar to that for G8, but significantly higher than that for G2 (24.8%). The percentage of step-like ICDs for G5, G3, and G4 are 63.5%, 55.4%, and 43.3%, respectively, indicating that removal of any of the three culture conditions (i.e., electrical stimulation, low Young's modulus, or substrate suspension) would cause a reduction in the percentage of step-like ICDs.

Table 3. Excitation Threshold for Cardiomyocyte Culture on Different Culture Days (Six Samples from Three Cell Isolations on 130 kPa Suspended Polydimethylsiloxane Substrate Measured as Mean ± SD)

	D4	*D5*	*D6*
ET (vol/cm)	3.3 ± 0.4	2.9 ± 0.3	2.6 ± 0.3

CM, cardiomyocyte; ET, excitation threshold; PDMS, polydimethylsiloxane; SD, standard deviation.

3D reconstruction of intercalated discs between rod-shaped cardiomyocytes

The results showed that, except for under G6, the cross-sectional shape of CMs under all test conditions was a flat oval with a ratio of cell width to height (the major axis to the minor axis) of ~4:1 and, equivalently, a cell height of ~3 μm (data not shown). However, CMs under G6 expressed an *in vivo*-like rod shape with a monolayer cell height of typically 6–12 μm. The 3D morphology of an ICD

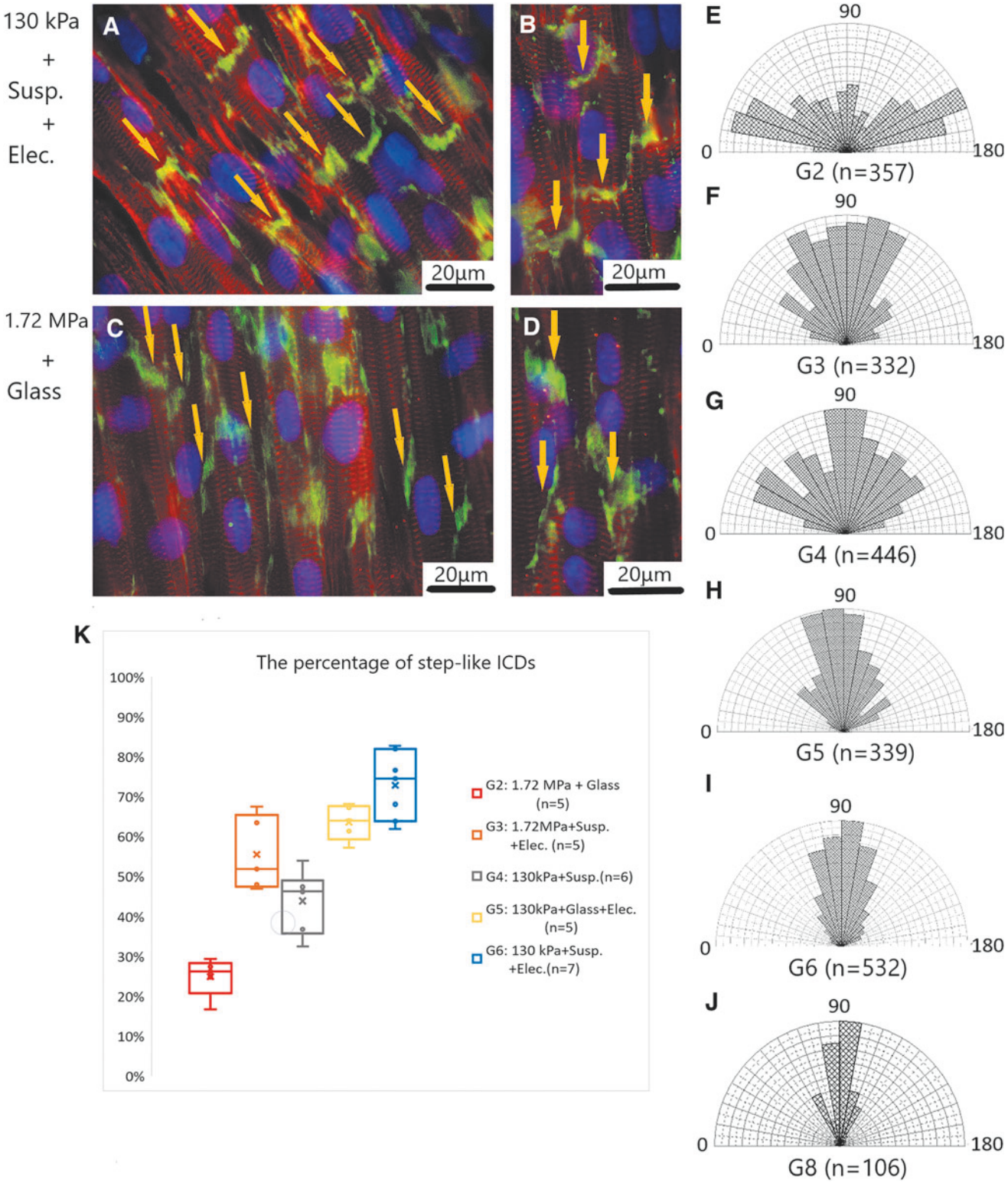

FIG. 4. Morphology of ICDs under different culture conditions. **(A–D)** Morphology of ICDs visualized by immunofluorescence staining: **(A, B)** Cultured on 130 kPa suspended substrate with electrical stimulation (G6): *pale orange arrows* show step-like ICDs; **(C, D)** culture on 1.72 MPa substrate attached on a coverglass without electrical stimulation (G2): *pale orange arrow* shows sigmoid ICDs. *Red*: α-actinin. *Green*: N-cadherin. *Blue*: nucleus. **(E-J)** ICD orientation: **(E)** under 1.72 MPa substrate attached on a coverglass without electrical stimulation, G2; **(F)** 1.72 MPa suspended substrate with electrical stimulation, G3; **(G)** 130 kPa suspended substrate without electric stimulation, G4; **(H)** 130 kPa substrate attached on a coverglass with electrical stimulation, G5; **(I)** 130 kPa suspended substrate with electrical stimulation, G6; and **(J)** heart tissue from adult rat, G8. **(K)** Box plot showing the percentage of step-like ICDs. *x* labeled mean, *middle line* labeled median. The differences between the result under G6 and each of those under G2 to G5 are all significant.

was reconstructed from the confocal-scanned image stack obtained from cell cultures under G6. Figure 5A and B demonstrates a typical reconstruction of ICDs from ICD images obtained in culture on 130 kPa suspended substrate with electrical stimulation (G6). The reconstructed ICD image includes two connected ICDs that formed between two side-to-side connected cells that were each joined end to end to another cell. The dimension of the ICD was ~7 μm in diameter, a typical dimension for neonatal rats (6 μm at birth; gradually increasing to 15 μm by 60 days)[16] and ~1 μm thick, a normal dimension for heart tissue. This shape of the ICD was similar to the 3D morphology obtained in rat heart tissue, the shape of which is a round disc between adjacent cells.

Electron transmission microscopy

Since only cultures under G6 expressed *in vivo*-like morphology, our TEM study was conducted on cultures under G6 only. TEM images obtained from rat CM cultures on 130 kPa suspended substrate with electrical stimulation (G6) fixed at culture Day 6 demonstrated a remarkable level of ultrastructural differentiation and step-like ICDs, comparable to those from adult tissue. Cells were aligned and elongated with highly organized myofibrils. Numerous mitochondria were positioned between myofibrils (Fig. 6A). Well-aligned sarcomeres were observed with visible Z lines and H, I, and A bands; an M line was faintly visible (Fig. 6C). These morphologic features are characteristic of those in rat myocardium (Fig. 6B, D). A transverse section of ICDs shows they are perpendicular to the longitudinal axis of myofibrils with a pleated appearance (Fig. 6E) as typically seen in a rat heart (Fig. 6F).

Sigmoid ICD formation process

To study the process of sigmoid ICD formation, we prepared multiple identical CM cultures under G2 and observed the culture development daily. Typical results for G2 are shown in Figure 7A–C. Before staining, the contractility of the culture was monitored microscopically, and those cultures that demonstrated minimum synchronous contraction (<50%) were chosen for staining. The orientation of ICDs was typically oblique to the axis of CM alignment (referred to hereafter as ''sigmoid ICDs''). Our sequential observation allowed us to speculate that the contact pattern may contribute to the formation of sigmoid ICDs: When a cell's center is not on the longitudinal axis of the grooves, the two corresponding curved portions on each cell touch and grow side by side to form a sigmoid contact profile to minimize contact energy (Fig. 7D).[17]

Blebbistatin test

Blebbistatin inhibits contraction. With the application of blebbistatin to the culture chamber with 130 kPa suspended substrate with electrical stimulation (G6), more sigmoid ICDs were observed than were observed without the addition of blebbistatin (image not shown), indicating that step-like ICD formation was inhibited.

Mechanical cyclic stretch

The results obtained from cyclic stretch without electrical stimulation (G7) showed that step-like ICDs did not form during 5% and 10% cyclic stretch: ICD inclination was much steeper with than without stretch (G4). It was even steeper than ICD inclination on 1.72 MPa substrate attached on a coverglass without electrical stimulation (G2) (Fig. 8, statistics not shown).

Discussion

In this study, ~70% of ICDs had a step-like profile and expression of an *in vivo*-like rod cell shape in CM cultures on microgrooved, 130 kPa, suspended PDMS substrate with electrical stimulation (G6). Our data suggest that under the three conditions of electrical stimulation, low Young's

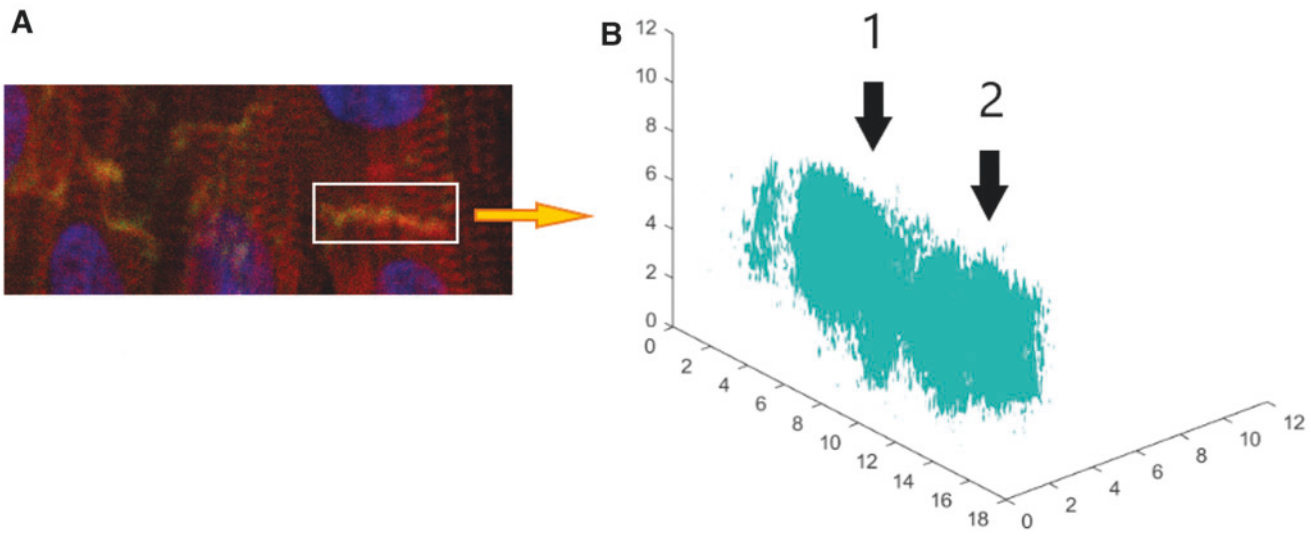

FIG. 5. A 3D reconstruction of two connected ICDs in culture on 130 kPa suspended substrate with electrical stimulation. **(A)** Immunofluorescence image recorded by confocal microscopy. **(B)** 3D view of the reconstructed ICD. Unit: μm. 3D, three-dimensional.

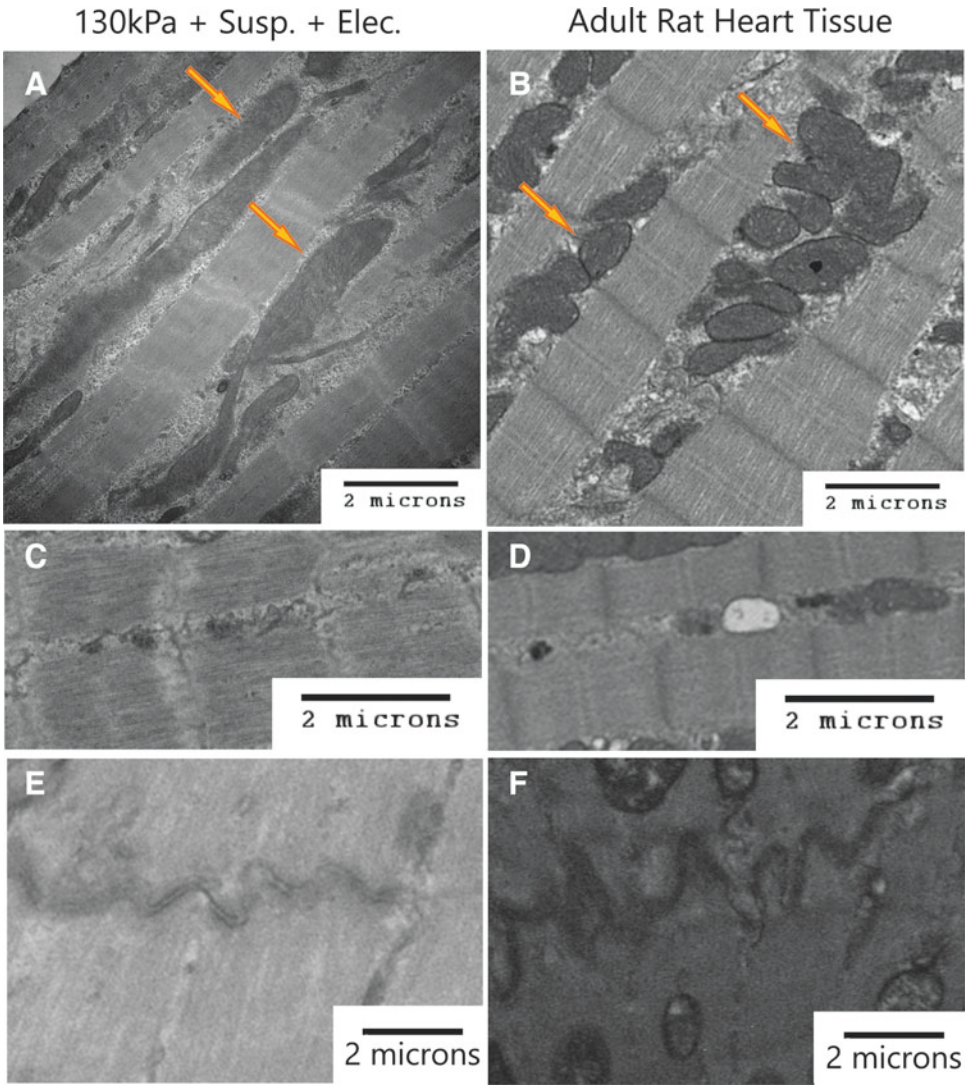

FIG. 6. Ultrastructural organization visualized by TEM imaging. **(A, C, E)** Representative TEM micrographs obtained from CM culture on 130 kPa suspended substrate with electrical stimulation (G6). **(B, D, F)** Representative TEM micrographs obtained from an adult rat heart. **(A, B)** Overview of myofibrils. *Orange arrows* point to mitochondria. **(C, D)** Ultrastructure of sarcomeres. **(E, F)** An ICD. TEM, transmission electron microscope.

modulus, and substrate suspension, the tugging force on ICDs generated by CM contraction on FA caused the formation of step-like ICDs.[18,19]

Our experimental observation of sigmoid ICD formation demonstrated that in the grooved substrate, the probability of forming sigmoid ICDs was high. As shown in Figure 9, however, when an inclined ICD was formed, the tugging forces exerted on the two sides of the ICD during synchronized contraction differed: The tugging force on the side with more sarcomeres was larger than the tugging force on the side with fewer sarcomeres, (Fig. 9B). This difference caused the ICDs to be stretched to an orientation perpendicular to the cell's direction of alignment. Under cyclic stretch without CM contraction, the forces were mainly from CM membranes that touched the substrate and exerted force equally on both sides of the ICDs. These forces did not cause step-like ICDs; in fact, their stretch inclined ICDs even more steeply.

The discussion above is correct for only conditions in which the number of sarcomeres on each side of the inclined ICD is different, as shown in Figure 9A and B. In our experiments (data not shown), we occasionally found that in the synchronous contraction region of a CM culture, inclined ICDs were consecutively lined up in parallel (i.e., inclined in the same direction) in a line of end-to-end connected CMs. This phenomenon occurred when by chance the original cell deposition arrangement allowed the consecutive cells to be formed at the same contact angle. Because the number of sarcomeres on each side was approximately the same, they exerted the same force and thus could not stretch the inclined ICD to become perpendicular to the longitudinal cell axis. The existence of this phenomenon supports our theory of stretch due to synchronized contraction caused by *in vivo*-like ICD orientation.

In our study, when we applied combined cyclic stretch and electrical stimuli, the results demonstrated that cellular viability was low (data not shown). When only a cyclic stretch was applied, our data demonstrated that the stretch-generated passive forces were neither physiological nor pathological; therefore, we did not extensively explore the combination. However, we did combine sustained static stretch (which mimicked hypertrophy) and electrical stimulation. We applied electrical stimulation to the cell culture under G6 from Day 3 (12–16 h earlier than the addition used

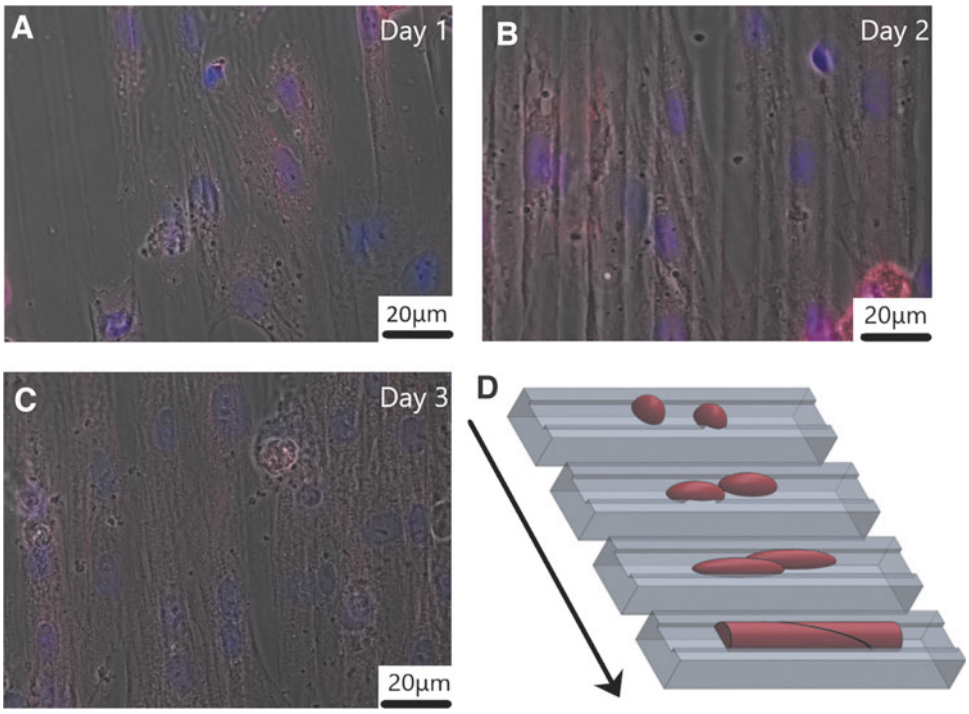

FIG. 7. The formation of sinusoidal ICDs on the first 3 days (**A–C**). *Red*: α-actinin; *Blue*: nucleus; *Gray*: Phase microscope imaging. **(D)** Cartoon demonstration of sigmoid ICD formation.

in the experiments we report in this study that were without any stretch) to Day 7; from Day 5 to 7, we also applied 5% static stretch. The *in vivo*-like ICDs that formed were not statistically different from those that formed under G6 without stretch (data not shown). This suggests that our system can be used as a hypertrophic model.

For 130 kPa suspended substrate with electrical stimulation (G6), the ICD morphology was *in vivo*-like (the percentage of step-like ICDs was closer to that of adult rat heart tissue than that of other test groups), and the ultrastructure of the ICDs was also similar to that in adult rat heart tissue. For example, the TEM result from the test group under G6 showed that the pleated appearance presented in transverse sections of ICDs (perpendicular to the longitudinal axis of the CM) was similar to that seen in adult rat heart tissue.[2] The major *in vivo*-like feature of the culture model under G6 was the 3D cell morphology: The CM expressed a rod-like shape, unlike CMs in other test groups in which the cross-sectional shape of a CM was a flat oval with a cell height around 3 μm. A 3D reconstruction of ICDs from a confocal image stack acquired from a culture model under G6 showed that the dimensions of the ICDs were ~6–12 μm in diameter (Fig. 5B), similar to a typical dimension obtained from neonatal rats.[16]

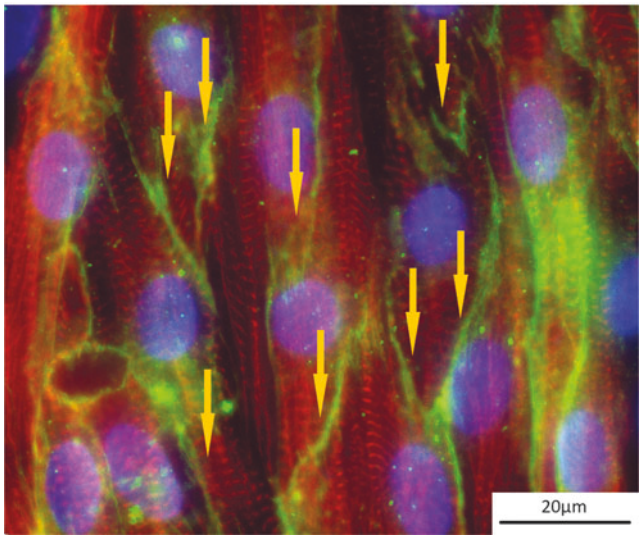

FIG. 8. Morphology of ICDs on cultures at 5% stretch on 130 kPa suspended substrate without electrical stimulation. *Yellow arrows* point to sigmoid ICDs. Scale bar = 20 μm. *Red*: α-actinin; *Green*: N-cadherin; *Blue*: nucleus.

It has been demonstrated extensively that actomyosin-based tugging forces play an important role in the formation of ICDs.[20–22] In the development of CMs, the myofibril contraction provides the tugging forces that promote and stabilize the formation of ICDs;[19,23,24] ICDs have been visualized as the terminal Z-discs of myofibrils and were seen to function as the terminal of the sarcomere.[18] To use a topographic technique (e.g., microgrooved substrate) to achieve cell alignment, Young's modulus of the substrate could not be tuned as low as that approaching the *in vivo* level. Consequently, during CM contraction, a cell's apical surface would contract much more strongly than the basal surface. As our long experience with CM culture confirms (data not shown), without concomitant contraction of equal strength of the apical and basal cell surfaces, the effects of the tugging forces were not sufficient to balance the outward pressure generated on the cell membrane and the cell/substrate adhesive force. The former caused a spherical contour of the cell membrane, and the latter caused the cell to spread on the substrate, forming a sheet. As a result, the typical appearance of the cell/cell contact interface would be

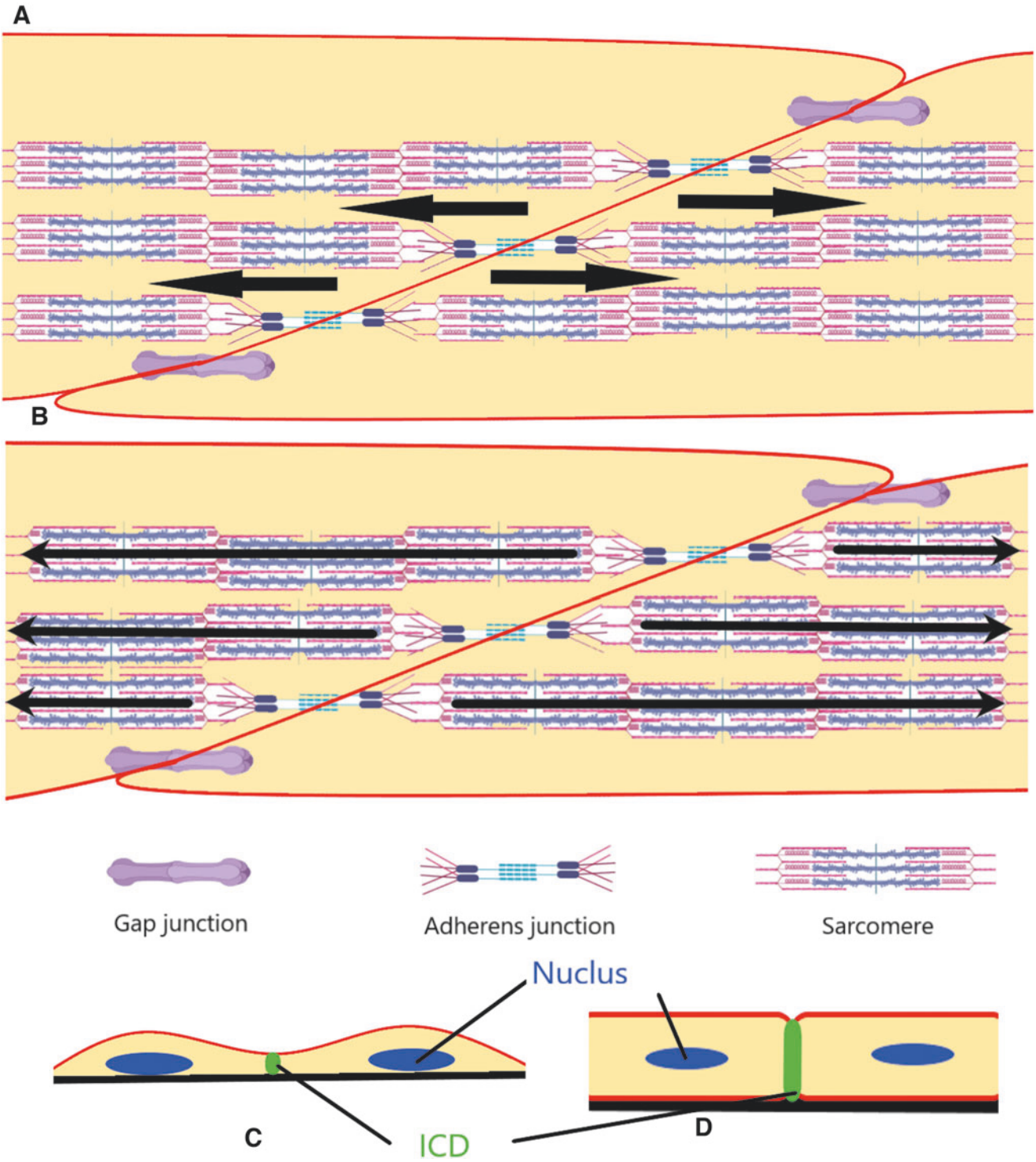

FIG. 9. Illustration of modeling. Modeling **(A)** mechanical stretch and **(B)** electrical stimulation. ICDs formed in random cell culture **(C)** and 130 kPa suspended substrate with electrical stimulation **(D)**.

as shown in Figure 9C. But, cell/cell contact in study has an appearance as shown in Figure 9D. Our experiment-based conceptualization is consistent with the mechanical analysis-based conclusion reported in the literature—that the height of a cell can be increased by a concomitant contraction of the apical and basal cell surfaces.[25] In our research report here, we used a suspended elastic substrate and filled the cell culture chamber with the minimum amount of medium—just enough for cell culture—so that the substrate was slack with scattered folds, not taut. Consequently, the effective stiffness of the substrate was lower than that of a taut substrate with the same Young's modulus, as in a heart muscle, in which crimps in the collagen fibrils decrease the effective stiffness of the tissue. In our culture

condition, the synchronous CM contraction was able to cause, as we observed, the substrate to contract with the cell culture, and thus a simultaneous contraction of equal strength of the apical and basal cell surfaces occurred. We postulate that this simultaneous contraction is the major reason for CMs cultured on our suspension substrate with low Young's modulus and under electrical stimulation to express a rod shape with disk-like ICDs.

In the future, these findings can be used to study the physiological and pathological features of ICDs. Not only does ICD morphology determine function, the morphology changes with the development of pathological conditions and causes malfunction of CMs. In the last decade in cardiomyopathy and gene deletion models, the transition of ICDs from a physiological morphology to a pathological morphology was found.[26,27] These morphological changes were correlated to their final effects on CM development and remodeling, which are regulated by cell/cell coupling mediated through ICDs. Consequently, studying physiological cell development and remodeling in a cell culture model requires the establishment of *in vivo*-like ICD morphology to assure physiological cell/cell coupling. For example, during hypertrophic cardiac cell remodeling, the insertion of sarcomeres (the basic unit of the contractile mechanism) is speculated to occur at the ICD.[28] In a culture model, an *in vivo*-like ICD enables actual mechanical interaction experienced by neighboring cells during hypertrophy. This mechanical interaction is thought to be an important causal factor in hypertrophic sarcomeric insertion.

In our study, we cultured neonatal rat CMs on PDMS, which is not suitable for transplant. However, this method could be combined with biodegradable materials to guide the formation of cell sheets with *in vivo*-like cell coupling for transplantation to damaged hearts.[29]

Disclosure Statement

No competing financial interests exist.

Funding Information

This study was partially supported by the National Institutes of Health through SC COBRE (P20RR021949 and P30GM131959), R01 funding (R01HL124782 and R01HL144927); and the National Science Foundation EPSCoR Program (OIA-1655740).

Supplementary Material

Supplementary Figure S1
Supplementary Video S1

References

1. Ladoux, B., Nelson, W.J., Yan, J., and Mege, R.M. The mechanotransduction machinery at work at adherens junctions. Integr Biol (Camb) **7,** 1109, 2015.
2. Forbes, M.S., and Sperelakis, N. Intercalated disks of mammalian heart—a review of structure and function. Tissue Cell **17,** 605, 1985.
3. Michaelson, J.E., and Huang, H. Cell-cell junctional proteins in cardiovascular mechanotransduction. Ann Biomed Eng **40,** 568, 2012.
4. Bursac, N., Parker, K.K., Iravanian, S., and Tung, L. Cardiomyocyte cultures with controlled macroscopic anisotropy: a model for functional electrophysiological studies of cardiac muscle. Circ Res **91,** e45, 2002.
5. McDevitt, T.C., Angello, J.C., Whitney, M.L., *et al*. In vitro generation of differentiated cardiac myofibers on micropatterned laminin surfaces. J Biomed Mater Res **60,** 472, 2002.
6. McDevitt, T.C., Woodhouse, K.A., Hauschka, S.D., Murry, C.E., and Stayton, P.S. Spatially organized layers of cardiomyocytes on biodegradable polyurethane films for myocardial repair. J Biomed Mater Res A **66A,** 586, 2003.
7. Thomas, S.P., Bircher-Lehmann, L., Thomas, S.A., *et al*. Synthetic strands of neonatal mouse cardiac myocytes. Struct Electrophysiol Properties **87,** 467, 2000.
8. Motlagh, D., Hartman, T.J., Desai, T.A., and Russell, B. Microfabricated grooves recapitulate neonatal myocyte connexin43 and N-cadherin expression and localization. J Biomed Mater Res A **67A,** 148, 2003.
9. Kim, D.-H., Lipke, E.A., Kim, P., *et al*. Nanoscale cues regulate the structure and function of macroscopic cardiac tissue constructs. Proc Natl Acad Sci U S A **107,** 565, 2010.
10. Luna, J.I., Ciriza, J., Garcia-Ojeda, M.E., *et al*. Multiscale biomimetic topography for the alignment of neonatal and embryonic stem cell-derived heart cells. Tissue Eng Part C Methods **17,** 579, 2011.
11. Palchesko, R.N., Zhang, L., Sun, Y., and Feinberg, A.W. Development of polydimethylsiloxane substrates with tunable elastic modulus to study cell mechanobiology in muscle and nerve. PLoS One **7,** e51499, 2012.
12. Li, Y.H., Huang, G.Y., Zhang, X.H., *et al*. Engineering cell alignment in vitro. Biotechnol Adv **32,** 347, 2014.
13. Palchesko, R.N., Zhang, L., Sun, Y., and Feinberg, A.W. Development of polydimethylsiloxane substrates with tunable elastic modulus to study cell mechanobiology in muscle and nerve. PLoS One **7,** e51499, 2012.
14. Berry, M.F., Engler, A.J., Woo, Y.J., *et al*. Mesenchymal stem cell injection after myocardial infarction improves myocardial compliance. Am J Physiol Heart Circ Physiol **290,** H2196, 2006.
15. Yang, H.X., Schmidt, L.P., Wang, Z.H., *et al*. Dynamic myofibrillar remodeling in live cardiomyocytes under static stretch. Sci Rep **6,** 20674, 2016.
16. Hirakow, R., Gotoh, T., and Watanabe, T. Quantitative studies on the ultrastructural differentiation and growth of mammalian cardiac-muscle-cells .1. The Atria and Ventricles of the Rat. Acta Anat **108,** 144, 1980.
17. Maitre, J.L., and Heisenberg, C.P. The role of adhesion energy in controlling cell-cell contacts. Curr Opin Cell Biol **23,** 508, 2011.
18. Li, Y., Merkel, C.D., Zeng, X.M., *et al*. The N-cadherin interactome in primary cardiomyocytes as defined using quantitative proximity proteomics. J Cell Sci **132,** jcs221606, 2019.
19. Liu, Z.J., Tan, J.L., Cohen, D.M., *et al*. Mechanical tugging force regulates the size of cell-cell junctions. Proc Natl Acad Sci U S A **107,** 9944, 2010.
20. Buckley, C.D., Tan, J.Y., Anderson, K.L., *et al*. The minimal cadherin-catenin complex binds to actin filaments under force. Science **346,** 600, 2014.
21. Charras, G., and Yap, A.S. Tensile forces and mechanotransduction at cell-cell junctions. Curr Biol **28,** R445, 2018.

22. Leckband, D.E., le Duc, Q., Wang, N., and de Rooij, J. Mechanotransduction at cadherin-mediated adhesions. Curr Opin Cell Biol **23,** 523, 2011.
23. Chopra, A., Tabdanov, E., Patel, H., Janmey, P.A., and Kresh, J.Y. Cardiac myocyte remodeling mediated by N-cadherin-dependent mechanosensing. Am J Physiol Heart Circ Physiol **300,** H1252, 2011.
24. Kresh, J.Y., and Chopra, A. Intercellular and extracellular mechanotransduction in cardiac myocytes. Pflugers Arch **462,** 75, 2011.
25. Mao, Y.L., and Baum, B. Tug of war-The influence of opposing physical forces on epithelial cell morphology. Dev Biol **401,** 92, 2015.
26. Kostetskii, I., Li, J., Xiong, Y., *et al*. Induced deletion of the N-cadherin gene in the heart leads to dissolution of the intercalated disc structure. Circ Res **96,** 346, 2005.
27. Laks, M.M., Morady, F., Adomian, G., and Swan, H. Presence of widened and multiple intercalated discs in the hypertrophied canine heart. Circ Res **27,** 391, 1970.
28. Wilson, A.J., Schoenauer, R., Ehler, E., Agarkova, I., and Bennett, P.M. Cardiomyocyte growth and sarcomerogenesis at the intercalated disc. Cell Mol Life Sci **71,** 165, 2014.
29. Masuda, S., Shimizu, T., Yamato, M., and Okano, T. Cell sheet engineering for heart tissue repair. Adv Drug Deliv Rev **60**, 277, 2008.

Address correspondence to:
Bruce Zhi Gao, PhD
Department of Bioengineering
Clemson University
401-2 Rhodes Hall
Clemson, SC 29634
USA

E-mail: zgao@clemson.edu

Received: March 19, 2020
Accepted: May 29, 2020
Online Publication Date: July 30, 2020